

## Lowest-energy structures and electronic properties of Na-Si binary clusters from ab initio global search

Linwei Sai, Lingli Tang, Jijun Zhao, Jun Wang, and Vijay Kumar

Citation: *The Journal of Chemical Physics* **135**, 184305 (2011); doi: 10.1063/1.3660354

View online: <http://dx.doi.org/10.1063/1.3660354>

View Table of Contents: <http://scitation.aip.org/content/aip/journal/jcp/135/18?ver=pdfcov>

Published by the [AIP Publishing](#)

---



## Re-register for Table of Content Alerts

Create a profile.



Sign up today!



# Lowest-energy structures and electronic properties of Na-Si binary clusters from *ab initio* global search

Linwei Sai,<sup>1,2,3</sup> Lingli Tang,<sup>1,2,3</sup> Jijun Zhao,<sup>1,2,a)</sup> Jun Wang,<sup>3</sup> and Vijay Kumar<sup>4</sup>

<sup>1</sup>College of Advanced Science and Technology, Dalian University of Technology, Dalian 116024, China

<sup>2</sup>Key Laboratory of Materials Modification by Laser, Ion and Electron Beams, Dalian University of Technology, Ministry of Education, Dalian 116024, China

<sup>3</sup>School of Mathematical Sciences, Dalian University of Technology, Dalian 116024, China

<sup>4</sup>Dr. Vijay Kumar Foundation, 1969 Sector 4, Gurgaon 122001, India

(Received 20 July 2011; accepted 24 October 2011; published online 14 November 2011)

The ground state structures of neutral and anionic clusters of  $\text{Na}_n\text{Si}_m$  ( $1 \leq n \leq 3$ ,  $1 \leq m \leq 11$ ) have been determined using genetic algorithm incorporated in first principles total energy code. The size dependence of the structural and electronic properties is discussed in detail. It is found that the lowest-energy structures of  $\text{Na}_n\text{Si}_m$  clusters resemble those of the pure Si clusters. Interestingly, Na atoms in neutral  $\text{Na}_n\text{Si}_m$  clusters are usually well separated by the  $\text{Si}_m$  skeleton, whereas Na atoms can form Na-Na bonds in some anionic clusters. The ionization potentials, adiabatic electron affinities, and photoelectron spectra are also calculated and the results compare well with the experimental data. © 2011 American Institute of Physics. [doi:10.1063/1.3660354]

## I. INTRODUCTION

Silicon is the most important semiconducting element and is the backbone of the modern microelectronics industry, while sodium is a typical simple metal with a nearly free valence electron. In the form of bulk solid, a few Na-Si alloy phases such as NaSi,  $\text{NaSi}_{14}$ , and  $\text{Na}_4\text{Si}_{23}$  have been reported,<sup>1</sup> and recently Na-Si binary phase diagram has been established.<sup>2</sup> In the past nearly 15 years, Na adsorption on Si surfaces has received considerable interest from both fundamental and technological points of view.<sup>3–16</sup> It has been found that the Na adsorption not only modifies the electronic and optical properties of a Si surface,<sup>4–8,16</sup> but it also results in the reconstruction of the surface structures.<sup>3,9,14,15</sup>

In cluster science, elemental clusters of both Si and Na have been the focus of intensive research;<sup>17–20</sup> however, much less attention has been paid to Na-Si mixed clusters. Similar to the case of silicon surfaces, it would be interesting to examine the effects of Na adsorption on the atomic and electronic structures of  $\text{Si}_n$  clusters. In a series of pioneer experiments, Kishi *et al.*<sup>21,22</sup> detected the geometric and electronic structures of neutral and anionic  $\text{Na}_m\text{Si}_n$  binary clusters up to  $n = 14$  and  $m = 5$  by means of mass spectroscopy, ionization potential, photoelectron spectroscopy, and reactivity with NO molecules. In addition to experiments, they also carried out *ab initio* MP2/6–31G\* calculations to compute the ground state configurations and electronic properties of  $\text{NaSi}_n$  and  $\text{NaSi}_n^-$  clusters with  $n = 1–7$ . Later, Yu *et al.*<sup>23</sup> have performed a detailed study on the ground state structures and electronic states of  $\text{NaSi}_6^-$  cluster using a combined technique with photoelectron spectroscopy and *ab initio* calculations.

Stimulated by the experimental progress, *ab initio* calculations have been performed by several groups to further ex-

plore the geometric and electronic properties of neutral and charged sodium-silicon binary clusters with up to two Na atoms and/or ten Si atoms.<sup>24–29</sup> In an early study by Wei *et al.*,<sup>24</sup> the most stable structures of  $\text{NaSi}_n$  and  $\text{NaSi}_n^+$  ( $n \leq 10$ ) clusters have been obtained from molecular dynamics simulations within the framework of density functional theory (DFT) and local density approximation (LDA). Li *et al.* optimized the ground state structures of semiconductor-alkali binary anion clusters  $\text{X}_n\text{A}^-$  ( $\text{X} = \text{Ge}$  and  $\text{Si}$ ;  $\text{A} = \text{K}$ ,  $\text{Na}$ , and  $\text{Li}$ ;  $n = 1–10$ ) using *ab initio* MP2 method and computed their vertical detachment energies (VDE).<sup>25</sup> Using B3LYP/6–31+G(d) method, Sporea *et al.*<sup>26,27</sup> investigated the equilibrium geometries and electronic properties (including adsorption energies, vertical and adiabatic ionization potentials, electric dipole moments, static dipolar polarizabilities, and population analysis) of  $\text{Na}_m\text{Si}_n$  and  $\text{NaSi}_n^+$  ( $n \leq 6$ ,  $m \leq 2$ ). Zhao *et al.*<sup>28</sup> explored the equilibrium geometries and electronic properties of neutral  $\text{Na}_m\text{Si}_n$  ( $m+n \leq 7$ ) clusters using DFT calculations at the B3LYP/6–311+G(d) level. Lin *et al.*<sup>29</sup> investigated the molecular structures, electron affinities, and dissociation energies of  $\text{NaSi}_n$  and  $\text{NaSi}_n^-$  ( $n \leq 10$ ) clusters using different DFT methods with DZP++ basis set.

Despite the above efforts, our current theoretical knowledge on Na-Si binary clusters is still rather limited due to the following reasons: (1) the previous studies were usually limited in the very small size range with up to only six to seven silicon atoms; (2) although the experiments of Kishi *et al.* provided data for the binary clusters with up to four Na atoms, most of the *ab initio* calculations included only one Na atom except for the work of Sporea who considered  $\text{Na}_2\text{Si}_n$  clusters up to  $n = 6$ ; (3) all cluster configurations in those previous works were constructed from some presumed structures and there was no global optimization for the ground state structures of these clusters. The last point is most critical since the potential energy surface (PES) of the clusters (in particular, the binary clusters) is so complicated that it is difficult to

<sup>a)</sup> Author to whom correspondence should be addressed. Electronic mail: zhaojj@dlut.edu.cn.

obtain their global minima and the best is to perform global search in an unbiased way.

To gain deeper insight into the ground state structures, bonding characteristics, and electronic properties of the Na-Si binary cluster system and to compare with more experimental data, in this paper we have systematically searched the lowest-energy structures of neutral and anionic  $\text{Na}_m\text{Si}_n$  ( $2 \leq n \leq 11$ ,  $0 \leq m \leq 3$ ) clusters using genetic algorithm (GA) incorporated within an *ab initio* code of the total energy calculation. The electronic properties including ionization potentials and electron affinities of these clusters have been computed and compared with experiments.

## II. COMPUTATIONAL METHODS

The unbiased global search of the most stable configurations of  $\text{Na}_m\text{Si}_n$  ( $1 \leq n \leq 11$ ,  $1 \leq m \leq 3$ ) clusters was carried out by using GA<sup>30,31</sup> as implemented in the DMol3 program.<sup>33</sup> The DFT calculations were performed with the double numerical basis including *d*-polarization function (DND) and generalized gradient approximation (GGA) with the Perdew-Burke-Enzerhof (PBE) functional.<sup>34</sup> Self-consistent field calculations were done with a convergence criterion of  $10^{-6}$  a.u. on the total energy. Orbital cutoff was set as 7.0 Å, and the cluster geometries were fully optimized without any symmetry constraint. For most situations, the zero point energy (ZPE) was not included in the total energy.

In the GA search, a number of initial configurations (16 isomers in this work) were generated from scratch. Any two individuals in this population were then chosen as parents to produce a child cluster via a “cut and splice” crossover operation,<sup>28</sup> followed by an optional mutation operation of 35% probability. Two types of mutations are used in this work: (1) give each atom of a cluster a small random displacement and (2) exchange the atom type of a pair of different types of atoms. The child cluster was then relaxed using DFT optimization. In order to keep the diversity of the populations, the locally stable child was selected to replace one of the individuals if they share the same value of inertia *I* (the tolerance for the *I* difference is less than  $0.04 \times$  atomic number); otherwise (the new structure has an inertia different from all existing isomer), replace the highest energy isomer by the new one. Here the inertia is defined as  $I = \sum m_i r_i^2$ , where  $r_i$  is the distance of the *i*th atom from cluster center and  $m_i$  is the mass of the *i*th atom. We defined the mass of element Si as 1 and the mass of element sodium as 2. For each cluster size, we performed 1000–3000 GA iterations to ensure that the global minimum on the PES is obtained. The number of GA iteration generally increases with cluster size, and relies on the specific chemical composition of the cluster. The details for the application of GA search in cluster physics can be found in the review articles.<sup>29–31</sup>

## III. LOWEST-ENERGY STRUCTURES OF $\text{Na}_n\text{Si}_m$ CLUSTERS

The lowest-energy structures of neutral and anionic  $\text{Na}_n\text{Si}_m$  clusters ( $1 \leq m \leq 11$ ,  $1 \leq n \leq 3$ ) are shown in



FIG. 1. The lowest energy structures of neutral  $\text{Na}_n\text{Si}$  and anionic  $\text{Na}_n\text{Si}^-$  clusters ( $1 \leq n \leq 3$ ). Yellow balls are for silicon and blue balls for sodium atoms.

Figs. 1–11. In the following, we discuss the details of these structures in the sequence of the number *m* of Si atoms. The Cartesian coordinates of all these lowest-energy structures are available online in the Cambridge Cluster Database.<sup>32</sup>

### A. $\text{Na}_n\text{Si}_1$ and $\text{Na}_n\text{Si}_1^-$

From our calculations, the equilibrium bond length of a NaSi dimer (quartet spin state) and  $\text{NaSi}^-$  anion are 2.724 Å and 2.944 Å, respectively. These are comparable to previous DFT calculations. For example, the Na-Si bond length was calculated to be 2.697 Å, 2.724 Å, 2.72 Å, 2.725 Å, and 2.742 Å in Refs. 21, 26–29, respectively, and for the anion it was calculated to be 2.84 Å<sup>22</sup> and 2.909 Å.<sup>29</sup> With two sodium atoms, the neutral  $\text{Na}_2\text{Si}$  cluster forms a Na-Si-Na chain with the Si atom in the middle (see Fig. 1). Our calculated Na-Si bond length is 2.739 Å and it is close to the value (2.711 Å) obtained by Kishi *et al.*<sup>22</sup> using MP2/6–31G(d) method as well as to the value of 2.70 Å obtained by Sporea *et al.*<sup>27</sup> at the level of B3LYP/6–31+G(d). The  $\text{Na}_2\text{Si}^-$  anion has an isosceles triangle configuration ( $C_{2v}$ ), with the waist and bottom edge lengths of 2.875 Å and 3.743 Å, respectively. The neutral  $\text{Na}_3\text{Si}$  cluster has a roof shape with  $C_s$  symmetry (see Fig. 1), in which two terminals Na atoms are separated by the middle Si-Na dimer and the Na-Si-Na-Na dihedral angle is 145.6°. The same structure was found by Zhao *et al.*<sup>28</sup> For  $\text{SiNa}_3^-$ , the three Na atoms bond with each other and form a triangle. The Si atom sits on the top of the  $\text{Na}_3$  triangle base, forming a trigonal pyramid ( $C_{3v}$ ). This is an interesting case as the number of valence electrons is 8, and it corresponds to electronic shell closure in a spherical Jellium model.

### B. $\text{Na}_n\text{Si}_2$ and $\text{Na}_n\text{Si}_2^-$

As shown in Fig. 2, the neutral  $\text{NaSi}_2$  cluster (with doublet spin state) adopts an isosceles triangle configuration. From our calculations, the Si-Na bond length is 2.922 Å and Si-Si bond length is 2.157 Å. Both the values compare well with the previously reported Si-Na bond lengths of 2.9 Å<sup>27</sup> and 2.905 Å,<sup>29</sup> and Si-Si bond length of 2.124 Å<sup>21</sup> and 2.121 Å.<sup>29</sup> The anionic  $\text{NaSi}_2^-$  cluster retains the isosceles

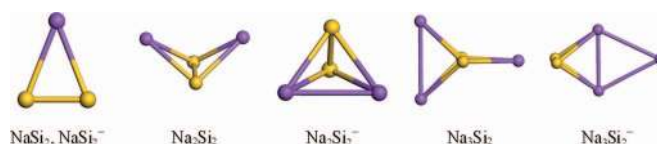


FIG. 2. The lowest energy structures of neutral  $\text{Na}_n\text{Si}_2$  and anionic  $\text{Na}_n\text{Si}_2^-$  clusters ( $1 \leq n \leq 3$ ). Yellow (blue) ball represent silicon (sodium) atoms.

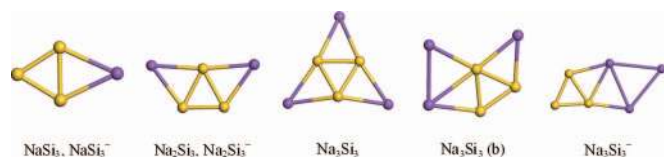


FIG. 3. The lowest energy structures of neutral  $\text{Na}_n\text{Si}_3$  and anionic  $\text{Na}_n\text{Si}_3^-$  clusters ( $1 \leq n \leq 3$ ).  $\text{Na}_3\text{Si}_3$  (b) denotes the most stable structure at room temperature. Yellow (blue) balls represent silicon (sodium) atoms.

triangle, and the Si-Na and Si-Si bond lengths become 2.841 Å and 2.186 Å, respectively, in agreement with the previous results of 2.783 Å and 2.188 Å in Ref. 22.

Similar to  $\text{Na}_3\text{Si}$ , the most stable structure of  $\text{Na}_2\text{Si}_2$  cluster has a roof shape (see Fig. 2) and the dihedral angle of Na-Si-Si-Na is  $106.1^\circ$ . The calculated Na-Si bond length in  $\text{Na}_2\text{Si}_2$  is 2.875 Å that is close to the previous values of 2.854 Å<sup>22</sup> and 2.87 Å.<sup>27</sup> Its Si-Si bond length is 2.193 Å from our calculation and 2.19 Å in Ref. 22. Again, analogous to  $\text{SiNa}_3^-$ , the  $\text{Na}_2\text{Si}_2^-$  cluster anion transforms into a trigonal pyramid with Na-Na, Si-Na, and Si-Si bond lengths of 3.422 Å, 3.024 Å, and 2.188 Å, respectively.

The lowest-energy configuration of  $\text{Na}_3\text{Si}_2$  cluster is an edge-capped distorted tetrahedron with  $C_{2v}$  symmetry (see Fig. 2), in which the three Na atoms are separated by the  $\text{Si}_2$  dimer. The same structure was reported by Zhao *et al.*<sup>28</sup> Interestingly, the  $\text{Na}_3\text{Si}_2^-$  anion also adopts a  $C_{2v}$  configuration as its neutral counterpart; however, the  $\text{Si}_2$  dimer goes to a side of the tetrahedron and the three Na form an equilateral triangle.

### C. $\text{Na}_n\text{Si}_3$ and $\text{Na}_n\text{Si}_3^-$

Interestingly, all of the neutral and anionic  $\text{Na}_n\text{Si}_3$  ( $n = 1-3$ ) clusters adopt planar configurations (see Fig. 3). The most stable structures of  $\text{NaSi}_3$  and  $\text{NaSi}_3^-$  share the same rhombus shape with some distortion ( $C_{2v}$  symmetry). Same structures were suggested previously in Refs. 26–29. From our calculations, the Na-Si bond length is 2.877 Å which is in line with the previous values of 2.88 Å in Ref. 27 and 2.874 Å in Ref. 29. For  $\text{NaSi}_3^-$ , the Na-Si bond length is shortened by

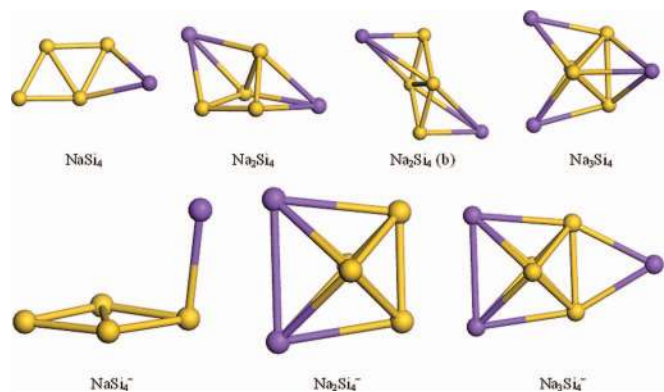


FIG. 4. The lowest energy structures of neutral  $\text{Na}_n\text{Si}_4$  and anionic  $\text{Na}_n\text{Si}_4^-$  clusters ( $1 \leq n \leq 3$ ).  $\text{Na}_2\text{Si}_4$  (b) denotes the most stable structure at room temperature. Yellow (blue) balls represent silicon (sodium) atoms.

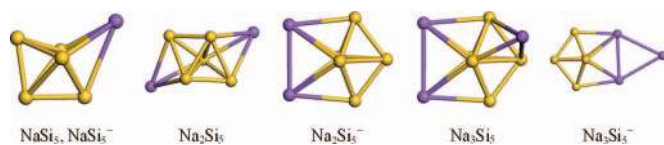


FIG. 5. The lowest energy structures of neutral  $\text{Na}_n\text{Si}_5$  and anionic  $\text{Na}_n\text{Si}_5^-$  clusters ( $1 \leq n \leq 3$ ). Yellow (blue) balls represent silicon (sodium) atoms.

0.031 Å, while Si-Si bond length is elongated by 0.143 Å and 0.008 Å with respect to the neutral cluster.

The ground state structure of both  $\text{Na}_2\text{Si}_3$  and  $\text{Na}_2\text{Si}_3^-$  is a trapezoid with  $C_{2v}$  symmetry; this is in agreement with the previous calculations in Refs. 22, 26–28. The Na-Si bond lengths in neutral  $\text{Na}_2\text{Si}_3$  cluster are 2.814 Å and 2.856 Å from our calculations, which compare well with the previous values of 2.80 Å and 2.84 Å in Ref. 27 and 2.829 Å and 2.842 Å in Ref. 22. The spin state of  $\text{Na}_2\text{Si}_3^-$  is doublet and its Na-Si bond lengths are 2.928 Å and 2.955 Å.

The planar structure of  $\text{Na}_3\text{Si}_3$  has  $C_{3v}$  symmetry; its three Na atoms are symmetrically separated by the central  $\text{Si}_3$  triangle tilted with a small off-plane angle. The previous calculations by Zhao *et al.*<sup>28</sup> proposed a different planar configuration for  $\text{Na}_3\text{Si}_3$  (shown as  $\text{Na}_3\text{Si}_3$  (b) in Fig. 3). However, we find this isomer to be 0.12 eV less stable than our lowest-energy  $C_{3v}$  structure. At room temperature of 298 K, after taking into account the Gibbs free energy calculated from the vibrational frequencies, this isomer predicted by Zhao *et al.* becomes more favorable.

The ground state configuration of  $\text{Na}_3\text{Si}_3^-$  is rather different from  $\text{Na}_3\text{Si}_3$  and it can be viewed as a planar combination of a  $\text{Na}_3$  triangle and a  $\text{Si}_3$  triangle. It is noteworthy that the sodium atoms tend to be well separated in the neutral  $\text{Na}_n\text{Si}_m$  clusters, whereas they can stay together in the negatively charged clusters. Natural population analysis (NPA) shows that each Na atom loses about 0.6 e in the neutral  $\text{Na}_3\text{Si}_3$  cluster. In the anionic  $\text{Na}_3\text{Si}_3^-$  cluster, the on-site charge for the two Na atoms bonded with  $\text{Si}_3$  triangle is  $\sim 0.29$  e, whereas the Na atom far away from Si carries a negative charge of about  $-0.35$  e. In short, in the anionic Na-Si clusters, there is less Coulomb repulsion between Na atoms with regard to the neutral clusters. In order to further check these results, we performed natural population analysis on NaSi and  $\text{NaSi}^-$  clusters. For the neutral NaSi cluster, Na atom loses 0.38 electrons, while Si atom gains 0.38 electrons. When the cluster carries a negative charge, the charge distribution on Na atom changes to  $-0.53$  e and Si atom is  $-0.47$  e. In other words, in the anionic clusters, there is less charge transfer from Na atom to Si atom due to the presence of the extra electron. In the larger anionic clusters with

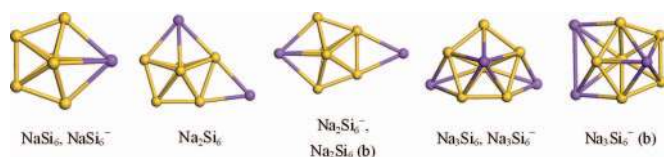


FIG. 6. The lowest energy structures of neutral  $\text{Na}_n\text{Si}_6$  and anionic  $\text{Na}_n\text{Si}_6^-$  clusters ( $1 \leq n \leq 3$ ). Yellow (blue) balls represent silicon (sodium) atoms.



FIG. 7. The lowest energy structures of neutral  $\text{Na}_n\text{Si}_7$  and anionic  $\text{Na}_n\text{Si}_7^-$  clusters ( $1 \leq n \leq 3$ ). Yellow (blue) balls represent silicon (sodium) atoms.

more than one Na atoms, less Coulomb repulsion between Na atoms with regard to the neutral clusters is anticipated and that has the tendency to favor clustering of Na atoms in some of the cases.

#### D. $\text{Na}_n\text{Si}_4$ and $\text{Na}_n\text{Si}_4^-$

The most stable structures of both  $\text{NaSi}_4$  and  $\text{NaSi}_4^-$  can be considered as a  $\text{Si}_4$  rhombus with one Na adatom (see Fig. 4). The Na atom is nearly located within the  $\text{Si}_4$  plane in the neutral cluster, and it almost sits perpendicular to  $\text{Si}_4$  plane (the angle between the Na-Si bond and the  $\text{Si}_4$  basal plane being  $83.8^\circ$ ) in the anionic case. Previously, a pyramid-like structure was predicted for  $\text{NaSi}_4$ ,<sup>26–29</sup> but it is less stable than our present structure by 0.095 eV. Moreover, the present structure was suggested as a metastable isomer in Ref. 26. Our most stable structure for  $\text{NaSi}_4^-$  is similar to the one obtained by Lin *et al.*,<sup>29</sup> but it is different from the prediction of a square pyramid by Kishi *et al.*<sup>22</sup>

The neutral  $\text{Na}_2\text{Si}_4$  cluster adopts a face-capped trigonal bipyramid structure with some distortion, in which two Na atoms are separated by the  $\text{Si}_4$  roof. This structure is the same as that obtained in Refs. 27 and 28, but it is different from a bi-capped rhombus structure ( $C_{2h}$ ) reported in Ref. 26, which is shown as  $\text{Na}_2\text{Si}_4$  (b) in Fig. 4. After including the Gibbs free energy at room temperature, this  $C_{2h}$  isomer becomes more stable than the face-capped trigonal bipyramid by 0.037 eV. For  $\text{Na}_2\text{Si}_4^-$ , the two Na and two Si atoms constitute an isosceles trapezoid. The remaining two Si atoms are located above and below the center of the trapezoid, forming a distorted octahedron.

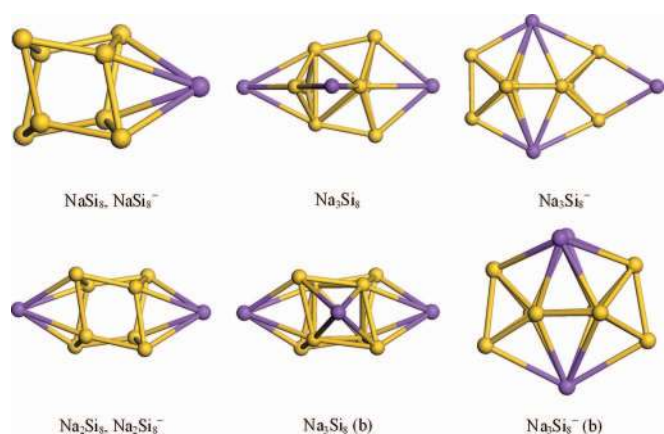


FIG. 8. The lowest energy structures and selected metastable isomers of neutral  $\text{Na}_n\text{Si}_8$  and anionic  $\text{Na}_n\text{Si}_8^-$  clusters ( $1 \leq n \leq 3$ ). Yellow (blue) balls represent silicon (sodium) atoms.

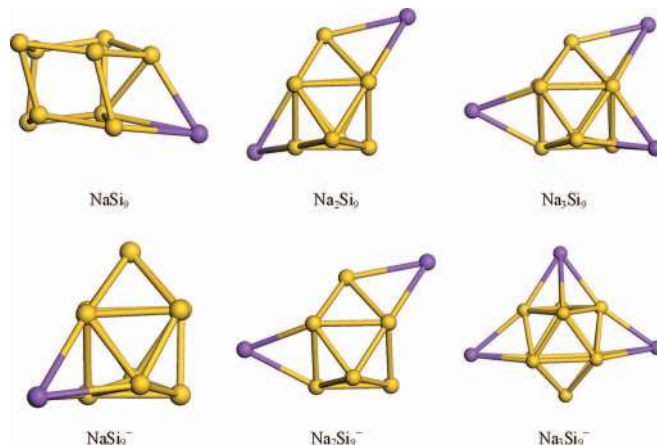


FIG. 9. The lowest energy structures of neutral  $\text{Na}_n\text{Si}_9$  and anionic  $\text{Na}_n\text{Si}_9^-$  clusters ( $1 \leq n \leq 3$ ). Yellow (blue) balls represent silicon (sodium) atoms.

In  $\text{Na}_3\text{Si}_4$ , the third Na atom locates on the face of the  $\text{Na}_2\text{Si}_4$  octahedron, whereas the two original Na atoms break the Na-Na bond and separate. Meanwhile, the third Na in  $\text{Na}_3\text{Si}_4^-$  is edge-capped on the  $\text{Na}_2\text{Si}_4^-$  structure without changing other parts of the configuration. The present structure of  $\text{Na}_3\text{Si}_4$  is the same as the one reported in Ref. 28.

#### E. $\text{Na}_n\text{Si}_5$ and $\text{Na}_n\text{Si}_5^-$

As shown in Fig. 5, the lowest-energy structures of  $\text{NaSi}_5$  and  $\text{NaSi}_5^-$  are similar with  $C_s$  symmetry and both can be viewed as a  $\text{Si}_5$  trigonal bipyramid face-capped with one Na. The same configuration was found before.<sup>26,28,29</sup> Similarly, the most stable structures of both  $\text{Na}_2\text{Si}_5$  and  $\text{Na}_2\text{Si}_5^-$  can be obtained by face-capping a trigonal bipyramid of  $\text{Si}_5$  with two Na atoms. In  $\text{Na}_2\text{Si}_5$  the two Na stay at the opposite faces, while the two Na atoms sit on one side and form a dimer in the case of  $\text{Na}_2\text{Si}_5^-$ . Our calculated structure of  $\text{Na}_2\text{Si}_5$  coincides with the one reported in Ref. 28, but it is slightly different from the  $C_s$  structure reported in Ref. 26 in which the two Na atoms are located on different faces of the trigonal bipyramid. The structures of Both  $\text{Na}_3\text{Si}_5$  and  $\text{Na}_3\text{Si}_5^-$  can

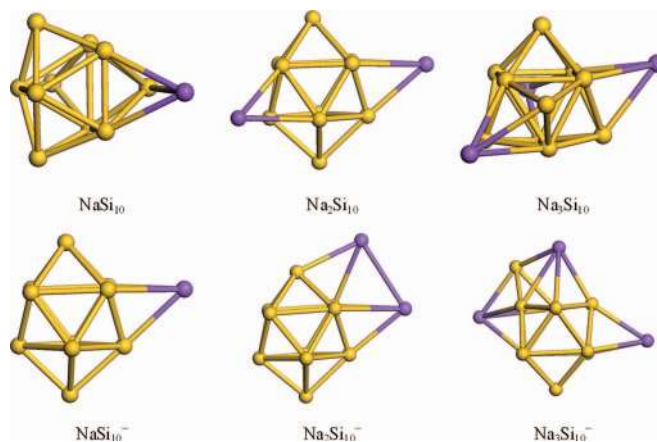


FIG. 10. The lowest energy structures of neutral  $\text{Na}_n\text{Si}_{10}$  and anionic  $\text{Na}_n\text{Si}_{10}^-$  clusters ( $1 \leq n \leq 3$ ). Yellow (blue) balls represent silicon (sodium) atoms.

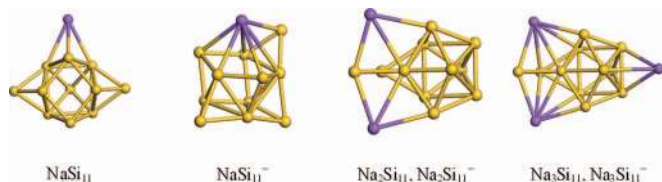


FIG. 11. The lowest energy structures of neutral  $\text{Na}_n\text{Si}_{11}$  and anionic  $\text{Na}_n\text{Si}_{11}^-$  clusters ( $1 \leq n \leq 3$ ). Yellow (blue) balls represent silicon (sodium) atoms.

be constructed by adding one Na atom on  $\text{Na}_2\text{Si}_5^-$  cluster. In the neutral case, the third Na atom is capped on one of the  $\text{Si}_3$  triangular face; while for the latter, the third Na atom is attached to two Na atoms, forming a  $\text{Na}_3$  triangle.

### F. $\text{Na}_n\text{Si}_6$ and $\text{Na}_n\text{Si}_6^-$

Starting from  $\text{NaSi}_6$  cluster, the lowest-energy structures are mainly based on those of bare Si clusters and the addition of Na atoms or extra charge does not result in significant change in the cluster configuration. Similar to  $\text{Si}_7$  cluster,<sup>35</sup> the structures of  $\text{NaSi}_6$  and  $\text{NaSi}_6^-$  are pentagonal bipyramids (see Fig. 6). The same configurations were found for  $\text{NaSi}_6$  (Refs. 26–29) and  $\text{NaSi}_6^-$  (Ref. 29) before. Both the ground state structures of  $\text{Na}_2\text{Si}_6$  and  $\text{Na}_2\text{Si}_6^-$  can be obtained by adding a bridged Na atom, but they are added at different places (see Fig. 6). Previously, it was argued that these two configurations are nearly degenerate with the energy difference of only 0.01 eV;<sup>26</sup> however, our calculations yield a difference of 0.11 eV. Again, the  $C_s$  structures of  $\text{Na}_3\text{Si}_6$  and  $\text{Na}_3\text{Si}_6^-$  are based on the pentagonal bipyramid of  $\text{Si}_7$ . In this case, one Na atom sits on the top of the bipyramid and the other two Na atoms cap on the two symmetric faces of the pentagonal bipyramid. The isomer of  $\text{Na}_3\text{Si}_6^-$  is 0.021 eV energy higher, and their difference is two Na atoms' arrangement.

### G. $\text{Na}_n\text{Si}_7$ and $\text{Na}_n\text{Si}_7^-$

The ground state  $C_{2v}$  structure of  $\text{NaSi}_7$  can be achieved by edge-capping a Na atom to the pentagonal bipyramid of  $\text{Si}_7$  cluster. However, with one extra charge, the anionic  $\text{NaSi}_7^-$  cluster undergoes significant structural change and transforms into a two-interlinked tetrahedral configuration. These two structures were previously proposed by Kishi *et al.*<sup>21</sup> and Lin *et al.*,<sup>29</sup> whereas Kishi *et al.* did not observe structural reconstruction for  $\text{NaSi}_7^-$ .<sup>22</sup>  $\text{Na}_2\text{Si}_7$  and  $\text{Na}_2\text{Si}_7^-$  share the same  $C_s$  configuration, which can be constructed from the most stable structure of bare  $\text{Si}_6$  cluster (i.e., a face-capped trigonal bipyramid)<sup>35</sup> with one edge-capped Si atom and two symmetrically side-capped Na atoms (see Fig. 7). Addition of one more Na atom on the face of  $\text{Si}_4$  rhombus of  $\text{Na}_2\text{Si}_7$  configuration leads to the most stable structure of  $\text{Na}_3\text{Si}_7$ . Surprisingly, the anion  $\text{Na}_3\text{Si}_7^-$  cluster adopts a completely different configuration (see Fig. 7) in which the three Na atoms constitute a triangle and six Si atoms separate into two parts: one with four Si atoms and another with two. Within the size

range considered, this is the only structure that Si atoms are separated.

### H. $\text{Na}_n\text{Si}_8$ and $\text{Na}_n\text{Si}_8^-$

It has been known that bare  $\text{Si}_8$  cluster possesses a tetra-capped tetrahedron configuration.<sup>35</sup> According to our calculations, the structures of all  $\text{Na}_n\text{Si}_8^-$  clusters except for  $\text{Na}_3\text{Si}_8^-$  can be obtained by face-capping a certain number of Na atoms on the tetra-capped tetrahedron of  $\text{Si}_8$  (see Fig. 8). The same configuration was reported for  $\text{NaSi}_8$  and  $\text{NaSi}_8^-$  previously by Lin *et al.*<sup>29</sup> In the  $D_{2d}$  configuration of  $\text{Na}_2\text{Si}_8$  and  $\text{Na}_2\text{Si}_8^-$ , the two Na atoms locate on the two sides of  $\text{Si}_8$ , while in  $\text{Na}_3\text{Si}_8$  cluster, the third Na atom sits in the middle. There are two nearly degenerate isomers for  $\text{Na}_3\text{Si}_8$ , that is, the third Na edge-capped on  $\text{Si}_8$  ( $C_s$ ) is more stable than the situation of face-capped Na ( $\text{Na}_3\text{Si}_8$  (b) in Fig. 8,  $C_2$  symmetry) by 0.001 eV. The structure of  $\text{Na}_3\text{Si}_8^-$  differs significantly from those of other clusters. It consists of two  $\text{Si}_4$  tetrahedra connected by two middle Na atoms and three Si-Si bonds; the third Na atom is edge-capped to one of the  $\text{Si}_4$  tetrahedra. A similar structure in which the third Na atom sits in the middle ( $\text{Na}_3\text{Si}_8^-$  (b) in Fig. 8) is only 0.002 eV less stable than the ground state one.

### I. $\text{Na}_n\text{Si}_9$ and $\text{Na}_n\text{Si}_9^-$

The lowest-energy structure of  $\text{NaSi}_9$  can be constructed from a distorted pentagonal bipyramid of  $\text{Si}_7$  by capping two Si atoms and one Na atom. This structure is the same as that in Ref. 29. With one extra charge, the anionic  $\text{NaSi}_9^-$  adopts a different configuration with  $C_s$  symmetry, which is obtained by adding one Na atom on a triangle face of tricapped trigonal prism of a bare  $\text{Si}_9$  cluster. This configuration is more stable than the cage structure proposed in Ref. 29 by 0.181 eV. Adding a sodium atom on the top of the trigonal prism leads to another metastable isomer of  $\text{NaSi}_9^-$ , which was also considered by Lin *et al.*<sup>29</sup> and it is 0.154 eV higher in energy than the lowest-energy one. The ground state structures of both  $\text{Na}_2\text{Si}_9$  and  $\text{Na}_2\text{Si}_9^-$  are obtained by adding one Na atom on the structure of  $\text{NaSi}_9^-$ , whereas the detailed arrangements of these two Na atoms are different in the neutral and anionic clusters (see Fig. 9). The lowest-energy structures of  $\text{Na}_3\text{Si}_9$  ( $C_s$ ) and  $\text{Na}_3\text{Si}_9^-$  ( $C_{2v}$ ) are based on tricapped trigonal prism of  $\text{Si}_9$  which is capped by three Na atoms in different ways (see Fig. 9). Except for  $\text{NaSi}_9$ , all other five structures share the same  $\text{Si}_9$  skeleton.

### J. $\text{Na}_n\text{Si}_{10}$ and $\text{Na}_n\text{Si}_{10}^-$

The bare  $\text{Si}_{10}$  cluster is known to adopt a tetracapped trigonal prism configuration, while the bicapped square antiprism is a metastable isomer.<sup>35,36</sup> From our GA search, the structures of neutral and anionic  $\text{Na}_n\text{Si}_{10}$  clusters are based on one of these two  $\text{Si}_{10}$  skeletons. Among them,  $\text{NaSi}_{10}$  and  $\text{Na}_3\text{Si}_{10}$  can be obtained by capping one or three Na atoms on the tetra-capped trigonal prism of  $\text{Si}_{10}$ . On the other hand, capping one to three Na atoms of the bicapped square antiprism of  $\text{Si}_{10}$

TABLE I. The IP and AEA of  $\text{Na}_n\text{Si}_m$  ( $n = 1-3$ ,  $m = 1-11$ ) clusters. The experimental values from Refs. 21 and 22 are given in parentheses for comparison.

Cluster	IP (eV)	AEA (eV)
NaSi	6.452(5.97 – 6.42)	0.964
NaSi <sub>2</sub>	7.122(>6.42)	1.483
NaSi <sub>3</sub>	6.843(>6.42)	1.717
NaSi <sub>4</sub>	6.102(5.91 – 6.42)	1.571(1.30 ± 0.05)
NaSi <sub>5</sub>	7.007(>6.42)	2.299(2.45 ± 0.05)
NaSi <sub>6</sub>	6.637(5.99 – 6.42)	1.913(1.90 ± 0.06)
NaSi <sub>7</sub>	5.854(5.45 ± 0.06)	1.901(1.94 ± 0.04)
NaSi <sub>8</sub>	6.993(>6.42)	2.704(2.44 ± 0.13)
NaSi <sub>9</sub>	6.442(>6.42)	2.706(2.66 ± 0.08)
NaSi <sub>10</sub>	6.174(5.77 ± 0.02)	2.578(2.57 ± 0.22)
NaSi <sub>11</sub>	6.371(5.99 – 6.42)	2.697(2.59 ± 0.25)
Na <sub>2</sub> Si	5.029	0.748
Na <sub>2</sub> Si <sub>2</sub>	5.818(5.60 ± 0.02)	0.647
Na <sub>2</sub> Si <sub>3</sub>	5.869(5.51 ± 0.07)	0.751
Na <sub>2</sub> Si <sub>4</sub>	5.964(5.42 ± 0.02)	1.386
Na <sub>2</sub> Si <sub>4</sub> b	5.499(5.42 ± 0.02)	1.386
Na <sub>2</sub> Si <sub>5</sub>	6.249(5.85 ± 0.07)	1.217(1.35 ± 0.05)
Na <sub>2</sub> Si <sub>6</sub>	5.617(5.37 ± 0.02)	1.137(1.46 ± 0.03)
Na <sub>2</sub> Si <sub>6</sub> b	5.788(5.37 ± 0.02)	1.435(1.46 ± 0.03)
Na <sub>2</sub> Si <sub>7</sub>	6.031(5.99 – 6.42)	1.343(1.61 ± 0.09)
Na <sub>2</sub> Si <sub>8</sub>	6.214(5.77 ± 0.02)	1.579(1.06 ± 0.04)
Na <sub>2</sub> Si <sub>9</sub>	6.271(5.99–6.42)	2.018(1.85 ± 0.05)
Na <sub>2</sub> Si <sub>10</sub>	6.219(5.99–6.42)	1.503(1.78 ± 0.02)
Na <sub>2</sub> Si <sub>11</sub>	6.095(5.99–6.42)	2.309
Na <sub>3</sub> Si	4.874	0.865
Na <sub>3</sub> Si <sub>2</sub>	4.121	1.040
Na <sub>3</sub> Si <sub>3</sub>	3.632(4.58 ± 0.02)	1.061
Na <sub>3</sub> Si <sub>3</sub> (b)	4.480(4.58 ± 0.02)	1.231
Na <sub>3</sub> Si <sub>4</sub>	5.316(5.01 ± 0.05)	1.142
Na <sub>3</sub> Si <sub>5</sub>	4.713(4.5 ± 0.02)	1.551(2.2 ± 0.04)
Na <sub>3</sub> Si <sub>6</sub>	5.580(5.23 ± 0.06)	1.633(1.51 ± 0.05)
Na <sub>3</sub> Si <sub>6</sub> <sup>−</sup> (b)		1.681(1.51 ± 0.05)
Na <sub>3</sub> Si <sub>7</sub>	4.830(4.7 ± 0.02)	1.958(2.41 ± 0.31)
Na <sub>3</sub> Si <sub>8</sub>	4.751(4.47 ± 0.04)	1.483(2.02 ± 0.14)
Na <sub>3</sub> Si <sub>8</sub> (b)	4.853(4.47 ± 0.04)	1.661(2.02 ± 0.14)
Na <sub>3</sub> Si <sub>8</sub> <sup>−</sup> (b)		1.581(2.02 ± 0.14)
Na <sub>3</sub> Si <sub>9</sub>	5.582(5.85 ± 0.06)	2.093(2.02 ± 0.14)
Na <sub>3</sub> Si <sub>10</sub>	4.955(4.67 ± 0.04)	1.700(1.95 ± 0.13)
Na <sub>3</sub> Si <sub>11</sub>	5.574(5.45)	1.987

leads to the most stable configurations of  $\text{NaSi}_{10}^-$ ,  $\text{Na}_2\text{Si}_{10}$ ,  $\text{Na}_2\text{Si}_{10}^-$ , and  $\text{Na}_3\text{Si}_{10}^-$ . It is noteworthy that one of the top Si atoms in the bicapped square antiprism skeleton of  $\text{Na}_3\text{Si}_{10}^-$  is replaced by a Na atom. Our theoretical prediction for the most stable structures of  $\text{NaSi}_{10}$  and  $\text{NaSi}_{10}^-$  agree with previous calculations by Lin *et al.*<sup>29</sup>

### K. $\text{Na}_n\text{Si}_{11}$ and $\text{Na}_n\text{Si}_{11}^-$

The bare  $\text{Si}_{11}$  cluster is known to adopt the distorted pentacapped trigonal prism configuration.<sup>36</sup> Capping one Na atom on this  $\text{Si}_{11}$  skeleton leads to the most stable structure of  $\text{NaSi}_{11}$ . However, the structure of anionic  $\text{NaSi}_{11}^-$  is significantly different. It is formed by a  $\text{NaSi}_8$  cage face-capped with three Si atoms (see Fig. 11). For the other four clus-

ters ( $\text{Na}_2\text{Si}_{11}$ ,  $\text{Na}_2\text{Si}_{11}^-$ ,  $\text{Na}_3\text{Si}_{11}$ , and  $\text{Na}_3\text{Si}_{11}^-$ ), the lowest-energy configurations share the same  $\text{Si}_9$  skeleton of tricapped trigonal prism. Moreover, the neutral and anionic clusters with two or three Na atoms have the same structure. Previously, there was no theoretical study on  $\text{Na}_n\text{Si}_{11}$  clusters and the sizes beyond.

## IV. SIZE-DEPENDENT ELECTRONIC PROPERTIES

To further explore the electronic properties of  $\text{Na}_n\text{Si}_m$  clusters, the vertical ionization energies (IPs) and adiabatic electron affinities (AEAs) of neutral  $\text{Na}_n\text{Si}_m$  clusters ( $1 \leq n \leq 3$ ,  $1 \leq m \leq 11$ ) are calculated. Our theoretical results are summarized in Table I, along with the experimental data by Kishi *et al.*<sup>21,22</sup> for comparison. Figure 12 plots the ionization energies of  $\text{NaSi}_n$ ,  $\text{Na}_2\text{Si}_n$ , and  $\text{Na}_3\text{Si}_n$  clusters as a function of the cluster size  $n$ . Here, the theoretical IP values for  $\text{Na}_3\text{Si}_3$  and  $\text{Na}_2\text{Si}_4$  were calculated using their most stable structures at room temperature, i.e., the isomers (b). Generally speaking, the agreement between theory and experiment is reasonable, and it is better for the  $\text{NaSi}_n$  and  $\text{Na}_3\text{Si}_n$  clusters.

For the IPs of  $\text{NaSi}_n$  clusters, both our first-principles calculations and experiments reveal that there are two peaks at  $n = 5$  and 8 and three valleys at  $n = 4, 7$ , and 10, which may be related to the relative stability of pure  $\text{Si}_n$  clusters. It is well known that  $\text{Si}_4$ ,  $\text{Si}_7$ , and  $\text{Si}_{10}$  are relatively stable.<sup>35</sup> Thus, the additional valence electron donated by the extra Na atom could be easily ionized, resulting in low IP values. For

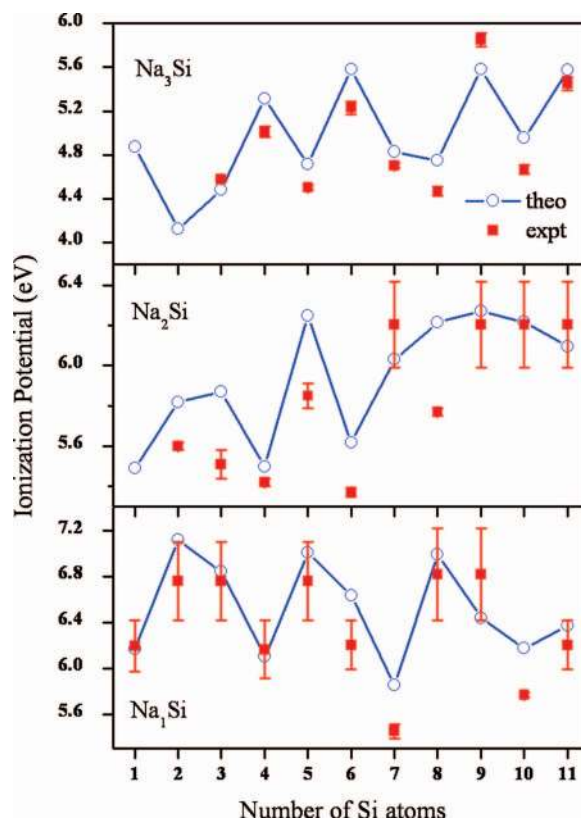


FIG. 12. Vertical ionization potentials of  $\text{NaSi}_n$ ,  $\text{Na}_2\text{Si}_n$ , and  $\text{Na}_3\text{Si}_n$  clusters ( $1 \leq n \leq 3$ ). Red squares with error bar are experimental data by Kishi *et al.*;<sup>21</sup> blue circles connected by solid line are our theoretical values.

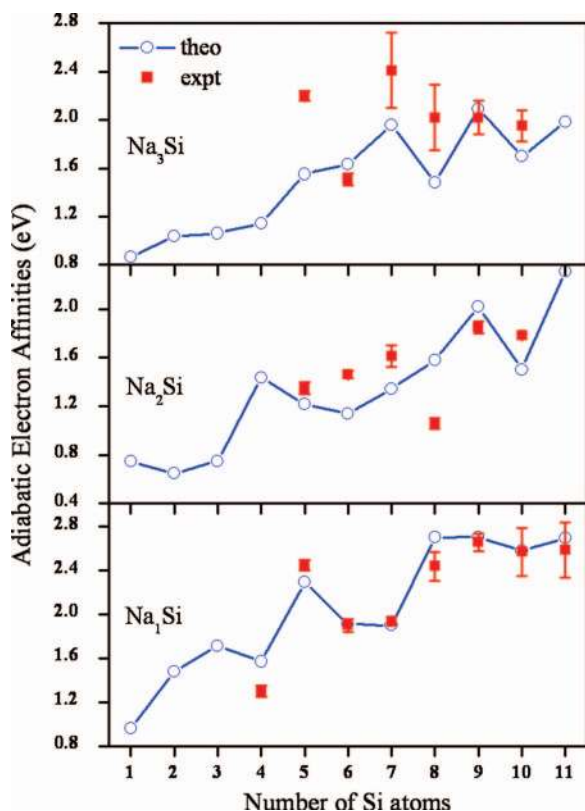


FIG. 13. Adiabatic electron affinities of  $\text{NaSi}_n$ ,  $\text{Na}_2\text{Si}_n$ , and  $\text{Na}_3\text{Si}_n$  clusters ( $n \leq 11$ ). Red squares with error bar are experimental data by Kishi *et al.*,<sup>22</sup> blue circles connected by solid line are our theoretical values.

$\text{Na}_2\text{Si}_n$ , our theoretical IP values are usually higher than the corresponding experimental data. Our calculations successfully reproduced the minimum at  $n = 6$ , but failed to describe the detailed size-dependent variation of IP data. Both theoretical and experimental IPs of  $\text{Na}_3\text{Si}_n$  clusters exhibit oscillations, with valleys at  $n = 3, 5, 7, 8$ , and  $10$  and peaks at  $n = 4, 6$ , and  $9$ .

Figure 13 displays the adiabatic electron affinities of  $\text{NaSi}_n$ ,  $\text{Na}_2\text{Si}_n$ , and  $\text{Na}_3\text{Si}_n$  clusters. Our theoretical calculations roughly agree with the experimental data,<sup>22</sup> especially for  $\text{NaSi}_n$ . For all of the  $\text{Na}_m\text{Si}_n$  clusters with three choice of  $m$ , the AEAs generally grow with cluster size  $n$  except for several local minima (e.g.,  $n = 4, 6$ , and  $7$  for  $\text{NaSi}_n$ ,  $n = 6$  and  $10$  for  $\text{Na}_2\text{Si}_n$ , and  $n = 8$  for  $\text{Na}_3\text{Si}_n$ ). For both IPs and AEAs, the discrepancy between theory and experiment might be partially explained by the temperature effect, that is, our theoretical prediction is made for the lowest-energy structures at zero temperature, while cluster beam experiments have been carried out with finite temperature at which some other low-lying isomer may become more favorable. For example, the IPs calculated using zero-temperature structures for  $\text{Na}_3\text{Si}_3$  and  $\text{Na}_2\text{Si}_4$  do not agree with experiment. However, for some clusters, inclusion of temperature effect via Gibbs free energy does not improve the agreement with experiments for IP or AEA. Thus, the remaining discrepancy between theoretical and experimental results (especially AEA) might also be attributed to the methodology (usage of DMol3 program, DND basis set, and GGA-PBE functional).

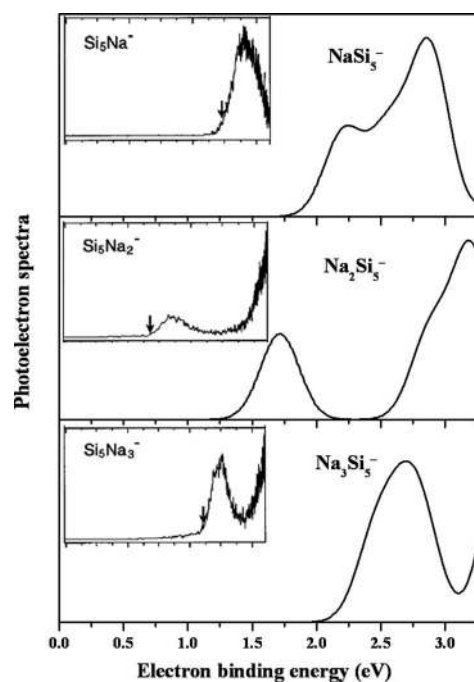


FIG. 14. Simulated photoelectron spectra of  $\text{Na}_n\text{Si}_5^-$  clusters ( $n = 1-3$ ). The experimental photoelectron spectra, taken from Ref. 22, are shown in inset using the same energy scale (from 0.0 to 3.25 eV).

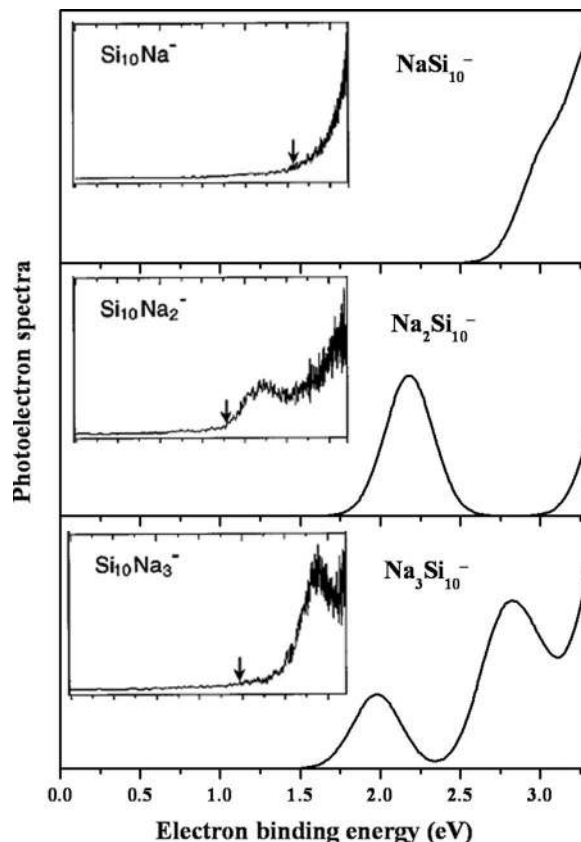


FIG. 15. Simulated photoelectron spectra of  $\text{Na}_n\text{Si}_{10}^-$  clusters ( $n = 1-3$ ). The experimental photoelectron spectra, taken from Ref. 22, are shown in inset using the same energy scale (from 0.0 to 3.25 eV).

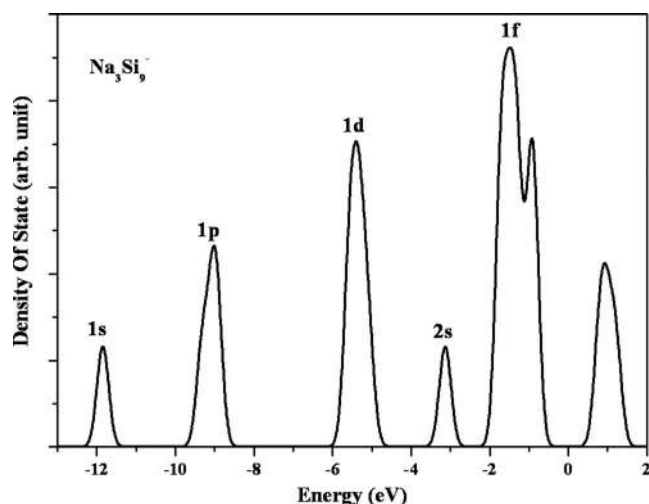


TABLE II. Binding energies (BEs) of neutral and anionic  $\text{Na}_n\text{Si}_m$  clusters ( $n = 1-3$ ,  $m = 1-11$ ).

Cluster	BE of neutral (eV/atom)	BE of anion (eV/atom)
NaSi	0.585	1.067
NaSi <sub>2</sub>	1.701	2.204
NaSi <sub>3</sub>	2.189	2.618
NaSi <sub>4</sub>	2.51	2.831
NaSi <sub>5</sub>	2.787	3.17
NaSi <sub>6</sub>	2.927	3.201
NaSi <sub>7</sub>	3.004	3.241
NaSi <sub>8</sub>	3.046	3.346
NaSi <sub>9</sub>	3.116	3.386
NaSi <sub>10</sub>	3.227	3.461
NaSi <sub>11</sub>	3.203	3.427
Na <sub>2</sub> Si	0.82	1.069
Na <sub>2</sub> Si <sub>2</sub>	1.738	1.9
Na <sub>2</sub> Si <sub>3</sub>	2.131	2.278
Na <sub>2</sub> Si <sub>4</sub>	2.32	2.551
Na <sub>2</sub> Si <sub>5</sub>	2.678	2.852
Na <sub>2</sub> Si <sub>6</sub>	2.747	2.89
Na <sub>2</sub> Si <sub>7</sub>	2.832	2.981
Na <sub>2</sub> Si <sub>8</sub>	2.940	3.098
Na <sub>2</sub> Si <sub>9</sub>	3.02	3.204
Na <sub>2</sub> Si <sub>10</sub>	3.107	3.232
Na <sub>2</sub> Si <sub>11</sub>	3.101	3.279
Na <sub>3</sub> Si	0.911	1.127
Na <sub>3</sub> Si <sub>2</sub>	1.532	1.740
Na <sub>3</sub> Si <sub>3</sub>	1.896	2.073
Na <sub>3</sub> Si <sub>4</sub>	2.203	2.367
Na <sub>3</sub> Si <sub>5</sub>	2.439	2.633
Na <sub>3</sub> Si <sub>6</sub>	2.538	2.719
Na <sub>3</sub> Si <sub>7</sub>	2.642	2.838
Na <sub>3</sub> Si <sub>8</sub>	2.769	2.904
Na <sub>3</sub> Si <sub>9</sub>	2.902	3.077
Na <sub>3</sub> Si <sub>10</sub>	2.937	3.068
Na <sub>3</sub> Si <sub>11</sub>	3.004	3.146

To further compare with experimental results,<sup>22</sup> we simulated the photoelectron spectra (PES) of the anionic  $\text{Na}_m\text{Si}_n^-$  clusters from their electronic density of states using the theoretical approach described in Ref. 37. As two representatives, the PES of anionic  $\text{Na}_n\text{Si}_5^-$  and  $\text{Na}_n\text{Si}_{10}^-$  clusters ( $n = 1-3$ ) are compared with experimental curves<sup>22</sup> in Figs. 14 and 15, respectively. Qualitatively, our theoretical simulation reproduces the features of experimental PES. For example, the first PES peak of  $\text{Na}_2\text{Si}_{10}^-$  is located at about 2.2 eV from experiment (Fig. 15), while our first-principles calculations predict a peak value of 2.18 eV. Similar agreement is found for other  $\text{Na}_m\text{Si}_n^-$  clusters, which demonstrates the validity of our theoretical calculations. Note that some low-intensity peaks are not distinctly shown in experimental spectra (e.g., the first peak in the PES of  $\text{Na}_3\text{Si}_{10}^-$ ) due to limitation of experimental resolution.

We also calculated the binding energy of  $\text{Na}_n\text{Si}_m$  ( $1 \leq n \leq 3$ ,  $1 \leq m \leq 11$ ) neutral and anionic clusters. The results are listed in Table II. It is noteworthy that the binding energy and IP have a decreasing trend with an increase in the number of Na atoms, though for  $\text{Na}_2\text{Si}_n$  in the larger size range the IP tends to have similar values as for  $\text{NaSi}_n$ .

FIG. 16. Electron density of states of the  $\text{Na}_3\text{Si}_9^-$  cluster (with Gaussian broadening of 0.15 eV). The electronic shells (1s, 1p, 1d, etc.) are labeled.

We also find that there are some correlation between the cluster stability and the number of valence electrons. For example, the  $\text{Na}_3\text{Si}_9^-$  cluster possesses a relatively large binding energy of 3.077 eV/atom and a largest AEA of 2.093 eV among  $\text{Na}_3\text{Si}_n^-$ , corresponding to high stability. This may be related to its forty valence electrons, which is a close-shell magic number predicted by the jellium model. The electronic states of the  $\text{Na}_3\text{Si}_9^-$  cluster are plotted in Fig. 16. Clearly, the molecular orbitals of valence electrons can be identified into groups that correspond to the discrete 1s, 1p, 1d, 2s, 1f shells, as predicted by the jellium model. The highest occupied molecular orbital-lowest unoccupied molecular orbital (HOMO-LUMO) gap (1.694 eV) of this anionic cluster is also appreciable.

## V. CONCLUSION

To summarize, unbiased searches using genetic algorithm incorporated within a first-principles approach were performed to obtain the lowest-energy configurations of neutral and anionic clusters of  $\text{Na}_n\text{Si}_m$  ( $1 \leq n \leq 3$ ,  $1 \leq m \leq 11$ ). Generally speaking, the ground state structures and geometry parameters from our theoretical calculations broadly agree with previous first-principles results wherever available, but the present work covers a broader range of cluster sizes. For  $\text{Na}_3\text{Si}_3$  and  $\text{NaSi}_9^-$ , we have obtained two new lowest-energy structures that are improvements over previous theoretical predictions. For neutral Na-Si clusters, Na atoms prefer to be separated from each other by the Si skeleton; however, in anionic clusters Na atoms can stay together and form Na-Na bonds. For smaller  $\text{Na}_n\text{Si}_m$  and  $\text{Na}_n\text{Si}_m^-$  clusters, the lowest-energy structures are sensitive to both Na-Si stoichiometry and charge state. For larger  $\text{Na}_n\text{Si}_m$  clusters with  $m > 7$ , addition of one Na atom or one extra charge would not result in significant change in the ground state structure. The electronic properties, including vertical ionization energies, adiabatic electron affinities, and photoelectron spectra, have been computed and compared with experimental

data. The satisfactory agreement between experiment and theory indicates the validity of our simulations.

## ACKNOWLEDGMENT

This work was supported by the Fundamental Research Funds for the Central Universities of China (No. DUT10ZD211) and the National Natural Science Foundation of China (No. 11134005).

- <sup>1</sup>P. Vallars, *Pearson's Handbook Desk Edition* (ASM International, Materials Park, OH, 1997), Vol. 2, and references therein.
- <sup>2</sup>H. Morito, T. Yamada, T. Ikeda, and H. Yamane, *J. Alloys Compd.* **480**, 723 (2009).
- <sup>3</sup>S. Olthoff, A. W. McKinnon, and M. E. Welland, *Surf. Sci.* **326**, 113 (1995).
- <sup>4</sup>Y. C. Chao, L. S. O. Johansson, and R. I. G. Uhrberg, *Surf. Sci.* **391**, 237 (1997).
- <sup>5</sup>J. J. Paggel, G. Neuhold, H. Haak, and K. Horn, *Surf. Sci.* **414**, 221 (1998).
- <sup>6</sup>C. Jordan, G. Marowsky, and H.-G. Rubahn, *Opt. Commun.* **120**, 98 (1995).
- <sup>7</sup>I. V. Kravetsky, G. Marowsky, and H. G. Rubahn, *Surf. Sci.* **474**, 47 (2001).
- <sup>8</sup>S. V. Rajkov, T. Nagao, V. G. Lifshits, and S. Husegawa, *Surf. Sci.* **493**, 619 (2001).
- <sup>9</sup>J. Zhang, V. G. Bordo, and H. G. Rubahn, *Solid State Commun.* **118**, 273 (2001).
- <sup>10</sup>K. Wu, Y. Fujikawa, T. Nagao, Y. Hasegawa, K. S. Nakayama, Q. K. Xue, E. G. Wang, T. Briere, V. Kumar, Y. Kawazoe, S. B. Zhang, and T. Sakurai, *Phys. Rev. Lett.* **91**, 126101 (2003).
- <sup>11</sup>E. Miyoshi, T. Iura, Y. Sakai, H. Tochihara, S. Tanaka, and H. Mori, *J. Mol. Struct. (THEOCHEM)* **630**, 225 (2003).
- <sup>12</sup>M. D'angelo, M. Konishi, I. Matsuda, C. Liu, S. Hasegawa, T. Okuda, and T. Kinoshita, *Surf. Sci.* **590**, 162 (2005).
- <sup>13</sup>C. C. Hwang, K. J. Kim, T. H. Kang, and B. Kim, *Surf. Sci.* **495**, 51 (2005).
- <sup>14</sup>J. R. Ahn, C. C. Hwang, and K.-S. An, *Vacuum* **81**, 226 (2006).
- <sup>15</sup>J. R. Ahn, S. H. Woo, J. H. Nam, and J. H. Park, *Surf. Sci.* **601**, 390 (2007).
- <sup>16</sup>A. K. S. Chauhan, R. Govind, S. M. Shivaprasad, *Thin Solid Films* **519**, 1012 (2010).
- <sup>17</sup>W. A. de Heer, *Rev. Mod. Phys.* **65**, 611 (1993).
- <sup>18</sup>*Clusters of Atoms and Molecules I: Theory, Experiment, and Clusters of Atoms*, edited by H. Haberland (Springer-Verlag, Berlin, 1994).
- <sup>19</sup>R. L. Johnston, *Atomic and Molecular Clusters* (Clarendon, Oxford, 2002).
- <sup>20</sup>F. Baletto and R. Ferrando, *Rev. Mod. Phys.* **77**, 371 (2005).
- <sup>21</sup>R. Kishi, S. Iwata, A. Nakajima, and K. Kaya, *J. Chem. Phys.* **107**, 3056 (1997).
- <sup>22</sup>R. Kishi, H. Kawamata, Y. Negishi, S. Iwata, A. Nakajima, and K. Kaya, *J. Chem. Phys.* **107**, 10029 (1997).
- <sup>23</sup>D. Yu Zubarev, A. N. Alexandrova, A. I. Boldyrev, L. F. Cui, X. Li, and L. S. Wang, *J. Chem. Phys.* **124**, 124305 (2006).
- <sup>24</sup>S. Wei, R. N. Barnett, and U. Landman, *Phys. Rev. B* **55**, 7935 (1997).
- <sup>25</sup>S. D. Li and G. M. Ren, *J. Chem. Phys.* **119**, 10063 (2003).
- <sup>26</sup>C. Sporea, F. Rabilloud, A. R. Allouche, and M. Aubert-Frécon, *J. Phys. Chem. A* **110**, 1046 (2006).
- <sup>27</sup>C. Sporea, F. Rabilloud, and M. Aubert-Frécon, *J. Mol. Struct. (THEOCHEM)* **802**, 85 (2007).
- <sup>28</sup>G. F. Zhao, J. M. Sun, X. Liu, L. J. Guo, and Y. H. Luo, *J. Mol. Struct. (THEOCHEM)* **851**, 348 (2008).
- <sup>29</sup>L. H. Lin, J. C. Yang, H. M. Ning, D. S. Hao, and H. W. Fan, *J. Mol. Struct. (THEOCHEM)* **851**, 197 (2008).
- <sup>30</sup>D. M. Deaven and K. M. Ho, *Phys. Rev. Lett.* **75**, 288 (1995).
- <sup>31</sup>J. J. Zhao and R. H. Xie, *J. Comput. Theor. Nanosci.* **1**, 117 (2004).
- <sup>32</sup>Cambridge Cluster Database. See <http://www-wales.ch.cam.ac.uk/CCD.html> for downloading Cartesian coordinates in present work.
- <sup>33</sup>B. Delley, *J. Chem. Phys.* **92**, 508 (1990); *J. Chem. Phys.* **113**, 7756 (2000).
- <sup>34</sup>J. P. Perdew, K. Burke, and M. Ernzerhof, *Phys. Rev. Lett.* **77**, 3865 (1996).
- <sup>35</sup>K. Raghavachari and C. M. Rohlfing, *J. Chem. Phys.* **89**, 2219 (1988).
- <sup>36</sup>C. M. Rohlfing and K. Raghavachari, *Chem. Phys. Lett.* **167**, 559 (1990).
- <sup>37</sup>J. Akola, M. Manninen, H. Hakkinen, U. Landman, X. Li, and L. S. Wang, *Phys. Rev. B* **60**, 11297 (1999).